Single-Molecule Identification of Coumarin-120 by Time-Resolved Fluorescence Detection: Comparison of One- and Two-Photon Excitation in Solution

L. Brand,[†] C. Eggeling,[†] C. Zander,[‡] K. H. Drexhage,[‡] and C. A. M. Seidel*,[†]

Max-Planck-Institut für Biophysikalische Chemie, Am Fassberg 11, 37077 Göttingen, Germany, and Institut für Physikalische Chemie, Universität-Gesamthochschule Siegen, Adolf-Reichwein-Strasse 2, 57068 Siegen, Germany

Received: November 8, 1996; In Final Form: March 17, 1997[⊗]

Using two-photon excitation (TPE) at 700 nm as well as one-photon excitation (OPE) at 350 nm, we applied confocal fluorescence microscopy to detect single Coumarin-120 molecules in the solvents water and triacetin. To study the behavior of Coumarin-120 under different excitation conditions, fluorescence lifetimes, multichannel scaler traces, and autocorrelation curves have been measured simultaneously. A signal-to-background ratio of 1300 was achieved for TPE due to a very low background level. The detection efficiency of TPE is limited by other competing nonlinear processes, in particular continuum generation in the solvent. The applicable laser intensity for OPE is limited by two-step photolysis of the dye as shown by fluorescence correlation spectroscopy (FCS). The time-resolved fluorescence signals were analyzed by a maximum likelihood estimator to identify the fluorophore through its characteristic fluorescence lifetime. The average fluorescence lifetimes 4.8 ± 1.2 ns in water and 3.3 ± 0.6 ns in triacetin are in good agreement with results obtained from separate measurements at higher concentrations.

1. Introduction

Detection of single molecules by laser-induced fluorescence opens new horizons for applications in analytical chemistry, biology, and medicine.[1−3] In previous studies of single molecules in liquids by one-photon excitation (OPE), small detection volumes V in sheath-flow cells ($V \approx 1$ pL)[4] or in a confocal microscope ($V \approx 1$ fL)[5] were used to reduce the background signal. This is caused mainly by the Raman emission of the solvent. Its intensity is proportional to the detection volume V.[4,5] Due to the considerable overlap of the fluorescence spectra of the used dyes with the Raman spectra, it appears to be necessary to use small volumes. To discriminate the fluorescence signal against the instantaneous Raman emission, time-resolved fluorescence detection has been applied previously.[4]

The necessity for the small detection volumes may be circumvented by two-photon excitation (TPE) of the fluorophore, because Rayleigh and Raman scattering occur in the near-IR and are well separated spectrally from the fluorescence signal in the UV/vis. The optimum size of the detection volume for TPE depends on several factors: (1) concentration of the fluorescent dye, (2) fluorescence background due to impurities, (3) diffusional transit time, in which an average number of fluorescence photons is emitted, and (4) photobleaching. TPE has been used successfully for single-molecule detection (SMD) of Rhodamine B in water,[6] SMD of diphenyloctatetraene trapped in a *n*-tetradecane matrix,[7] fluorescence correlation spectroscopy (FCS) in cells[8] as well as in fluorescence microscopy,[9] and many others. A particular feature of TPE is its dependence on the square of the intensity. This permits selective excitation in the focal plane. This inherent sectioning effect avoids excessive photodamage of the fluorophore as well as excitation of impurities anywhere else in the sample.

So far, dyes have been used for single-molecule detection and identification[3,5,11−15] by OPE, which have their S_0-S_1 absorption maxima in a wavelength region ranging from green to near-IR i.e., fluoresceins,[3] boradipyrromethane dyes,[3] rhodamines,[4,13] oxazines,[15] and carbocyanines.[11] To our knowledge, single dye molecules with a S_0-S_1 absorption maximum in the UV have not yet been detected in solution by OPE.

A comparison of OPE for Coumarin-120 and rhodamines shows that in contrast to rhodamines Coumarin-120 has a large Stokes shift of 6750 cm^{-1} which allows a good spectral separation of the fluorescence from Raman scattering. This property makes Coumarin-120 a good candidate for SMD due to a low background level. A serious problem of most coumarins is their low photochemical stability. The quantum yield of photobleaching on low-intensity OPE is on the order of $10^{-3}-10^{-4}$,[16b] which is 2 orders of magnitude larger than the photobleaching yield of rhodamines.[38] An additional problem of OPE in the UV region may be two-step photolysis at high excitation intensities.[16]

The main task in SMD in liquids is to maximize the number of detected fluorescence photons and to minimize at the same time the background signal, because the statistical accuracy of dye characterization via fluorescence spectra or lifetimes depends on the number of collected fluorescence photons.[10] Therefore, it is a prerequisite for successful SMD with TPE that the TPE cross section of the fluorophore is sufficiently high; i.e., it should be possible to reach the saturation for dye excitation before other limiting nonlinear effects (see below) or heating of the solvent occur. In this view coumarins are ideal candidates for SMD by TPE, because they have high TPE cross sections of approximately 20×10^{-50} cm^4 s in the wavelength region around 700 nm.[21,22]

Recent advances in SMD have made it possible to characterize single molecules through their fluorescence properties. Single molecules in solution have been identified on the basis of their fluorescence emission spectrum[13] or of their fluorescence lifetime.[14,15] Hence, molecular recognition which allows the characterization of particular molecular states will be a major step toward the study of single-molecule dynamics. To detect individual states in equilibrium for a single molecule of interest by time-resolved fluorescence spectroscopy, a fluorescent probe

* Corresponding author. E-mail: cseidel@gwdg.de.
[†] Max-Planck-Institut für Biophysikalische Chemie.
[‡] Universität-Gesamthochschule Siegen.
[⊗] Abstract published in *Advance ACS Abstracts,* May 1, 1997.

S1089-5639(96)03729-2 CCC: $14.00

whose fluorescence lifetime is influenced by these dynamics must be attached to the molecule. A dye appropriate to detect and to characterize nucleobases in their DNA environment is Coumarin-120. If this dye is coupled to nucleotides, its fluorescence is quenched in a typical way by each nucleobase, resulting in nucleobase-specific fluorescence lifetimes. The four nucleobase-specific fluorescence lifetimes range from 1.9 to 5.3 ns.[18] This suggests applications in projects for single-molecule DNA sequencing.[1,2] Furthermore, coumarin dyes are frequently used as laser dyes[17] and as fluorescent labels in life sciences (e.g., AMCA). In view of the versatile use of coumarins, we decided to study the efficiency of SMD by OPE as well as TPE. In the present article we compare both excitation techniques, calculate the signal-to-background ratio, and show the limitations with respect to SMD of Coumarin-120. Important techniques for data analysis are fluorescence correlation spectroscopy and time-resolved fluorescence spectroscopy. We present a maximum likelihood algorithm which allows the identification of single Coumarin-120 molecules via their characteristic fluorescence lifetime.

2. Experimental Section

2.1. Setup. The experimental setup has been described in principle recently.[14] A mode-locked titanium:sapphire laser (Mira 900F, Coherent, Palo Alto, CA) pumped by an argon ion laser (Innova 415, Coherent) was used as excitation source at 700 nm for TPE and frequency doubled at 350 nm for OPE. The pulse width τ_p was approximately 300 fs at a repetition rate of 76 MHz. Possible group-delay dispersion effects on τ_p are not taken into account. For TPE the laser beam was prefocused by a lens ($f = 200$, 250, or 300 mm depending on the type of experiment) and coupled into an epiilluminated microscope by a dichroic short pass beam splitter (Laseroptik, Garbsen, Germany). An oil-immersion objective (SPlanapo 100×, NA = 1.4 oil; 160 mm optics, Olympus, Japan) was used to focus the laser beam onto the sample. For OPE the diameter of the laser beam was adjusted by a telescope. The beam was coupled into an epiilluminated microscope by a dichroic long pass beam splitter (400 DCLP; AHF Analysentechnik, Tübingen, Germany) and focused onto the sample by a glycerol-immersion objective (Ultrafluar 100×, NA = 1.2; infinity optics, Zeiss, Germany). For OPE and TPE the laser spot sizes were determined by fluorescence correlation spectroscopy using a diffusion coefficient $D = 8 \times 10^{-6}$ cm^2 s^{-1} for Coumarin-120 in water.[31] The laser power was adjusted by inserting different neutral density filters (Lambda Physik, Göttingen, Germany) and by two polarizers. The mean quasi-CW power at the sample was measured by a power meter (Fieldmaster, Coherent). Fluorescence was collected by the same objective (Olympus-SPlanapo) and passed through a pinhole (diameter 100 μm) in the image plane. For the Zeiss-Ultafluar objective we used a tubus lens with $f = 150$ mm. To suppress scattered excitation light, a dichroic band-pass filter (395−547 nm; Schott, Mainz, Germany) was placed in front of the detector (bialkali photomultiplier tube R5600P-03 (Hamamatsu Photonics, Shimokanzo, Japan)). The amplified detector signal was registered by three different devices: (1) a PC adapter counter (CTM-05, Keithley, Taunton, MA) for multichannel scaler traces of the signal, (2) a real-time correlator card (ALV-5000/E, ALV, Langen, Germany), and (3) a time-correlated single-photon counting (TSC) setup in the reversed mode with conventional NIM modules interfaced with a PC board (ATDIO32F, National Instruments), which allows a sequence of measurements of fluorescence decay curves with a fixed photon number. The solutions for single-molecule experiments of Coumarin-120 (Lambda Physik, Göttingen) were prepared by diluting 10^{-6} M stock solutions with the appropriate amount of solvent, double-distilled water or triacetin (Aldrich, Steinheim, Germany), down to the required concentration of 1×10^{-11} M. During the measurements the dye solutions were contained in a depression of a microscope slide with a volume of approximately 100 μL (Roth, Karlsruhe, Germany) and covered by a conventional cover glass. For OPE the microscope slides were illuminated by UV light before use to bleach contaminations.

2.2. Fluorescence Correlation Spectroscopy. Fluorescence correlation spectroscopy (FCS) was used as a tool to obtain precise statistical characteristics with respect to an average molecule number in the detection volume and an average diffusion time (i.e., spot size of laser focus).[1,29] Furthermore, the analysis of the dependence of the average molecule number N in the detection volume on the laser excitation intensity provides information on the photostability of the fluorescent dye molecules. The fluctuations of the fluorescence photon flow $F_P(t)$ were analyzed by the normalized intensity autocorrelation function $G(t_c)$, where t_c is the correlation time. The spatial distribution of the detected fluorescence depends on two parameters: (1) the excitation volume defined by the photon flux E_P in case of OPE or of the squared laser photon flux E_P^2 in case of TPE; (2) the collection efficiency function CEF of the detection system given by the size and the position of the pinhole. The resulting molecule detection efficiency MDE can be approximated by a 3-dimensional Gaussian fluorescence distribution $W(x,y,z) = \exp(-2(x^2 + y^2)/\omega_0^2) \exp(-2(z^2)/z_0^2)$ in the case of OPE[23] or by the squared distribution $W^2(x,y,z)$ in the case of TPE. If translational diffusion is the only noticeable process that causes the measured fluorescence flow $F_P(t)$ to fluctuate about an average value $\langle F_P(t)\rangle$, $G(t_c)$ is given by eq 1.[29,30]

$$G(t_c) = \frac{\langle F_P(t)\, F_P(t+t_c)\rangle}{\langle F_P(t)\rangle^2} = 1 + \frac{(1 - I_B/S)^2}{\sqrt{8N}}\left(\frac{1}{1 + (t_c/\tau_{Dx})}\right) \times \left(\frac{1}{1 + (w_0/z_0)^2(t_c/\tau_{Dx})}\right)^{1/2} \quad (1)$$

To correct the decrease of the amplitude $G(t_c = 0)$ caused by the background signal, the ratio of the background intensity I_B to the total signal intensity S ($S = F + I_B$) is included in eq 1.[30] Depending on the type of excitation, different characteristic times for diffusion τ_{Dx} in the excitation volumes are obtained: τ_{D1} for OPE ($x = 1$) and τ_{D2} for TPE ($x = 2$). Using a three-dimensional Gaussian intensity distribution for the MDE, the radial 1/e^2 radius ω_0 is related to the different characteristic times for diffusion τ_{Dx} via the translational diffusion coefficient D: $\tau_{D1} = \omega_0^2/4D$ and $\tau_{D2} = \omega_0^2/8D$.

3. Results and Discussion

3.1. Intensity Dependence of OPE and TPE Fluorescence. To obtain information necessary for an optimized single-molecule detection, we studied the dependence of the fluorescence signal on the excitation intensity, in particular (1) dependence of the signal-to-background ratio (S/B) on the excitation energy[36] and (2) deviations from the expected linear and quadratic relations to obtain information on the saturation of the optical transition and on photobleaching. Furthermore,

FCS was applied to determine the diameter of the laser beam in the sample plane and to investigate photobleaching. In the subsequent analysis of OPE and TPE it appears advantageous to describe the laser intensity I (W cm^{-2}) by the photon flux E_P (cm^{-2} s^{-1}) and the time-averaged collected fluorescence signal by the fluorescence photon flow F_P (s^{-1}).[19]

3.1.1. OPE Analyzed by Time-Correlated Single-Photon Counting. In the absence of saturation of the S_0-S_1 transition and photobleaching of a fluorescent dye, eq 2 gives the linear dependence of the collected time-averaged fluorescence photon flow F_P on the quasi-CW photon flux $E_{P,qcw}$,

$$F_P = \alpha\sigma c N_A \phi_F (E_{P,qcw}) \beta \int_v W(x,y,z)\, dx\, dy\, dz \qquad (2)$$

where α is a unitless constant which is proportional to the detection efficiency of the system, σ is the one-photon absorption cross section, c is the molar concentration of the fluorescent dye, N_A is Avogadro's constant, Φ_F is the fluorescence quantum yield, and β is a unitless constant for the relation between F_P and $E_{P,qcw}$. The spatial distribution of the detected fluorescence photons for a OPE can be described by a three-dimensional Gaussian distribution $W(x,y,z)$ (see section 2.2). In the case of OPE β is expected to be equal to 1.

Using time-resolved fluorescence detection, we investigated the intensity dependence of the OPE fluorescence on a 5×10^{-8} M aqueous solution of Coumarin-120 at an excitation wavelength of 350 nm. Varying the excitation intensity by 5 orders of magnitude, the time-resolved signal decays were measured for a fixed integration time. Each integrated signal curve was fitted by a single-exponential fluorescence decay to calculate the fluorescence photon flow F_P. In Figure 1a the fluorescence signal is plotted versus the quasi-CW photon flux $E_{P,qcw}$ according to eq 2 (open circles). For comparison, the signal of pure water is also given in Figure 1a (filled diamonds). For all laser intensities the fluorescence decay curves show a single-exponential decay with a fluorescence lifetime of 5.0 ns, which is typical for Coumarin-120 in water.[18]

Three characteristic regions of the fluorescence signal can be distinguished in Figure 1a: (1) By fitting the data to $y = ax^\beta$ for a small photon flux, we obtain $\beta = 1.04$ as expected from eq 2. (2) At a photon flux of 7×10^{22} cm^{-2} s^{-1} a rather sharp maximum of the fluorescence signal is reached. (3) A further increase of the excitation energy results in a dramatic decrease of the fluorescence. On the other hand, the background signal measured on pure water increases linearly over the entire investigated intensity range. We attribute the main part of the background signal to luminescence of the optical setup, mainly the objective, because the signal is also present in the absence of sample. The use of microscope objectives other than the Zeiss Ultrafluar resulted in higher background signals.

The deviation of the fluorescence signal from the linear power dependence at higher intensities is not caused by saturation of the S_0-S_1 transition. This follows from the calculation of the fraction S_{1av} of dye molecules being in the S_1 state using a steady-state solution in a kinetic molecular energy scheme with three levels:[36] electronic ground state S_0, first electronic excited singlet state S_1, and triplet state T_1. According to this calculation, the portion S_{1av} of the molecules in the S_1 state is only 2%[37] at the maximum of the fluorescence signal. This indicates that the S_0-S_1 transition is far away from saturation. It is well-known for UV excitation (photon energy 3.2 eV) that the absorption of a second photon of molecules in the first electronic excited singlet or triplet state, S_1 and T_1, produces a higher energetic S_n and T_n state (two-step excitation) which couples quite efficiently with ionic states in polar solvents such as water. Hence two- or multistep absorption processes open additional channels for photobleaching at high intensities.

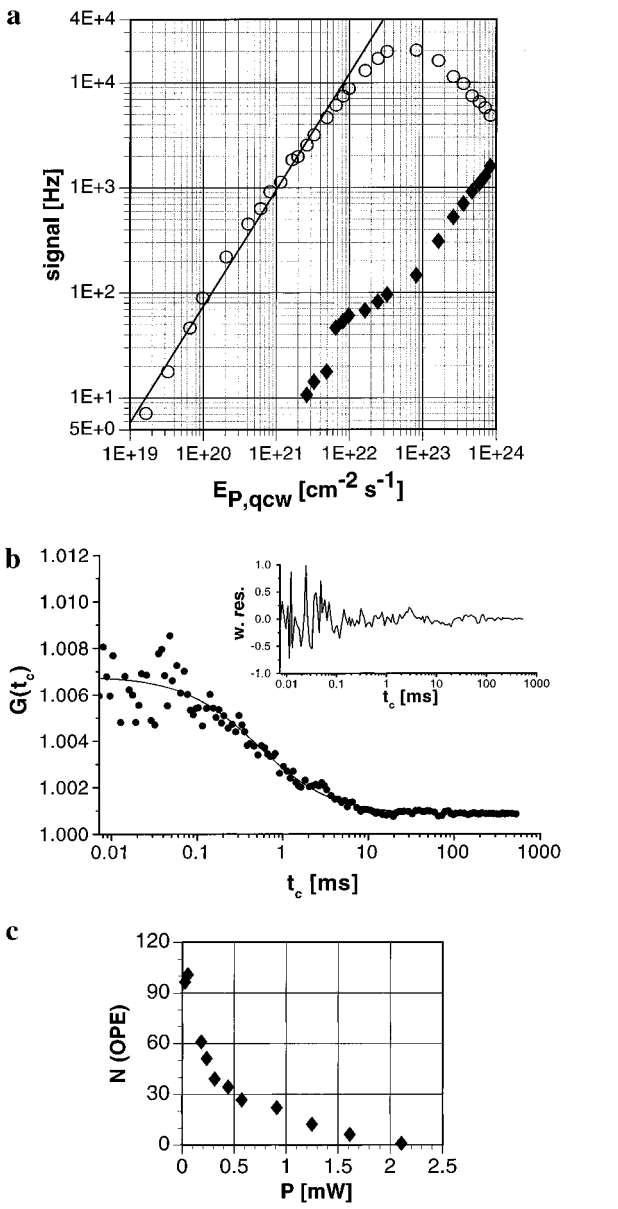

Figure 1. (a) Average fluorescence signal (open circles) of Coumarin-120 (5×10^{-8} M in water) and background signal of water (filled diamonds) at an excitation wavelength of 350 nm. The signal is plotted versus the mean quasi-CW photon flux $E_{P,qcw}$ according to eq 2. Fit according to eq 2 with $\beta = 1.04$. The detection volume was characterized by FCS for low intensities: $\tau_{D1} = 0.08$ ms ($\omega_0 = 0.51$ μm); $z_0/\omega_0 = 2.5$ μm. (b) Fluorescence autocorrelation curve $G(t_c)$ of 10^{-9} M Coumarin-120 in water with OPE ($P = 182$ μW) for an expanded excitation volume: Recorded data (black dots) and fitted function (eq 1) with weighted residuals (inset: w. res.).[30] Parameters of the fit with a background intensity of 9.4 kHz and a total signal intensity of 24 kHz: base line = 1.001, $N = 61$, $\tau_{D1} = 0.5$ ms ($\omega_0 = 1.34$ μm), $z_0/\omega_0 = 8.7$. (c) Dependence of the average number N(OPE) of Coumarin-120 molecules in the detection volume on the applied laser power P for OPE determined by FCS. The different fluorescence autocorrelation curves were recorded under the same optical conditions and with the same dye solution. N(OPE) is calculated from the amplitude $G(t_c{=}0)$ of the fits according to eq 1 (see (b) for parameters).

By transient absorption spectroscopy (TRABS) of Coumarin-120[16] and related coumarins,[39] it was shown that the S_1 as well as the T_1 state absorbs also in the wavelength region of the S_0-S_1 transition; i.e., there is a certain probability for a two-step laser photolysis. Using an aqueous solution of Coumarin-120 (10^{-5} M), the dependence of the transient spectra on the

laser power[16] was studied (data not shown). Two different lasers were used for an excitation with a repetition rate smaller than 1 Hz: (1) a XeF excimer laser (pulse width $\tau_p = 20$ ns, wavelength 351 nm, $E_{P,pk}$(saturation) $= 5 \times 10^{24}$ cm^{-2} s^{-1}); (2) a frequency-tripled Nd:YAG laser laser (pulse width $\tau_p =$ 30 ps, wavelength 354 nm, $E_{P,pk}$(saturation) $= 9 \times 10^{26}$ cm^{-2} s^{-1}). For both lasers we detected the characteristic spectra of the two-step photolysis products at higher pulse energies: solvated electrons (absorption maximum at 720 nm) and dye radical cations. The concentration of the photolysis products showed a quadratic dependence on the pulse energy. Compared to TRABS, the photon flux ($E_{P,pk}$(saturation) $= 3 \times 10^{27}$ cm^{-2} s^{-1}) at the focal plane necessary for an efficient SMD is of the same order of magnitude. Therefore, we applied FCS to investigate the hypothesis of two-step photolysis in SMD by studying the dependence of the average number of unbleached dye molecules N in the detection volume on the laser power P. We expanded the radius of the excitation volume by a factor 2.6 compared to Figure 1a in order to increase the probability of observing photobleaching due to a longer transit time through the excitation volume. A typical correlation curve $G(t_c)$ for the expanded excitation volume ($\omega_0 = 1.34$ μm, $\tau_{D1} = 0.5$ ms) is given in Figure 1b.

According to eq 1, the average number of dye molecules N(OPE) was calculated from the amplitude $G(t_c{=}0)$ corrected for the background signal. Figure 1c shows the dependence of N(OPE) on the laser power P. A drastic drop in N(OPE), decreasing from 100 to 1, is detectable already for low P.

In conclusion, we have evidence that the efficiency of OPE of Coumarin-120 is limited by a two-step photoionization at higher excitation intensities.

3.1.2. TPE Analyzed by Time-Correlated Single-Photon Counting. In the absence of saturation and photobleaching of the fluorescent dye, eq 3 (see Appendix) describes the quadratic dependence of the collected time-averaged fluorescence photon flow F_P on the quasi-CW photon flux $E_{P,qcw}$,[20−22]

$$F_P = \alpha\delta c N_A \frac{\phi_F}{2}\frac{0.588}{\tau_p f}(E_{P,qcw})\beta\int_v W_2(x,y,z)\,dx\,dy\,dz \quad (3)$$

where α, c, and N_A are used analogous to eq 2, δ is the two-photon absorption cross section, and β is an unitless constant for the relation between F_P and $E_{P,qcw}$. (For TPE β should be equal to 2.) The factor $^1/_2$ takes into account that two photons are needed for excitation. The periodic train of excitation pulses is characterized by the repetition rate f and the excitation pulse width τ_p. The spatial distribution of the detected fluorescence photons for TPE is described by a squared three-dimensional Gaussian distribution $W^2(x,y,z)$ (see section 2.2). Using time-resolved fluorescence detection, the intensity dependence of the TPE fluorescence of Coumarin-120 was investigated with an excitation wavelength of 700 nm. Varying the excitation intensity by 3 orders of magnitude, the time-resolved signal decays were measured for a fixed integration time. In Figure 2a F_P is plotted versus the quasi-CW photon flux $E_{P,qcw}$ according to eq 3 (open circles). For comparison, the peak photon flux $E_{P,pk}$, defined as $E_{P,qcw} \times 0.88/(f\tau_p)$,[21] is given on the upper x-axis. A maximum peak photon flux $E_{P,pk}$ of 3×10^{31} cm^{-2} s^{-1}was applied.

Again, three characteristic regions of the signal are observed: (1) if the data are fitted according to $y = ax^\beta$ for a small photon flux, we obtain $\beta = 1.99$ as expected from eq 3. The fluorescence decay curves can be described by a single-exponential decay with the fluorescence lifetime of 5.0 ns typical for Coumarin-120 in water.[18] (2) Saturation of fluorescence

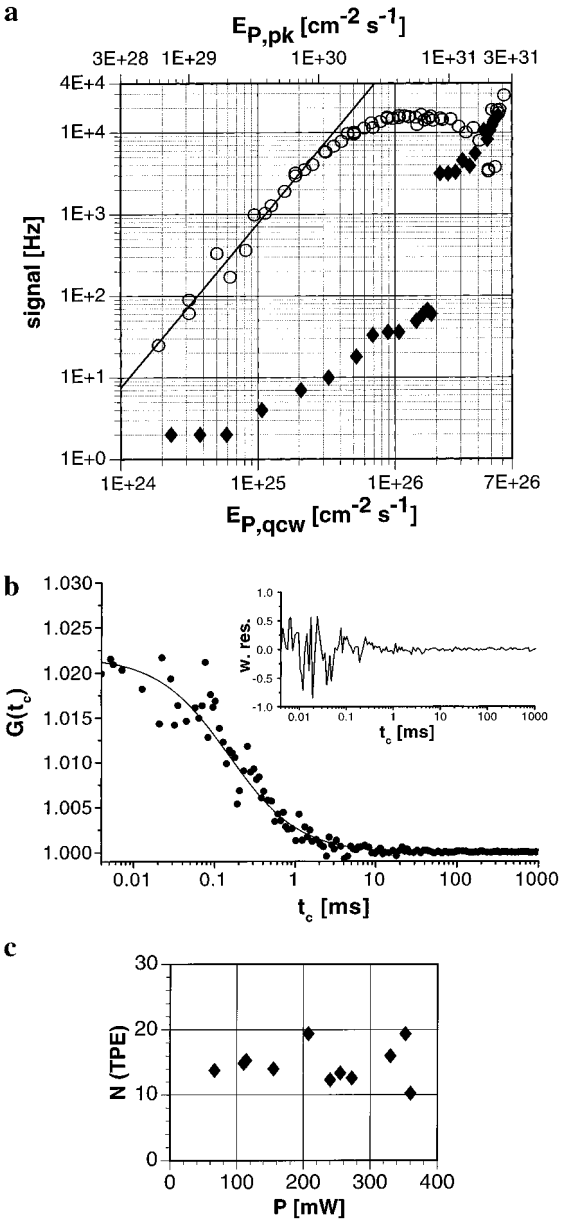

Figure 2. (a) Average fluorescence signal (open circles) of an aqueous solution of Coumarin-120 (5×10^{-8} M) and the signal of pure water (filled diamonds) due to background signal and continuum generation (excitation wavelength 700 nm). The signal is plotted versus the mean quasi-CW photon flux $E_{P,qcw}$. Fit according to eq 3 for a small photon flux with $\beta = 1.99$. For comparison, the peak photon flux $E_{P,pk}$ is given on the upper scale, assuming $\tau_p = 300$ fs and ×a6 =76 MHz. The detection volume was characterized at a photon flux $E_{P,qcw} = 2 \times 10^{26}$ cm^{-2} s^{-1}: $\tau_{D2} = 43$ μs ($\omega_0 = 0.53$ μm), $z_0/\omega_0 = 8.5$. (b) Fluorescence autocorrelation curve $G(t_c)$ for an aqueous solution of Coumarin-120 (10^{-9} M) with TPE ($P = 207.5$ mW): recorded data (black dots) and fitted curve (eq 1) with weighted residuals (inset: w. res.)).[30] Parameters of the fit with a background intensity of 0.26 kHz and a total signal intensity of 4.36 kHz: base line = 1.0, $N = 19.4$, $\tau_{D2} = 150$ μs ($\omega_0 =$ 0.98 μm), $z_0/\omega_0 = 10.7$. (c) Dependence of the average number N(TPE) of Coumarin-120 molecules in the detection volume on the applied laser power P for TPE determined by FCS. The different fluorescence autocorrelation functions were recorded under the same optical conditions and with the same dye solution. N(TPE) is calculated from the amplitude of the fits to $G(t_c)$ according to eq 1 (see Figure (b) for parameters).

begins to occur at a quasi-CW photon flux of 2×10^{25} cm^{-2} s^{-1}. (3) If the quasi-CW photon flux exceeds 2×10^{26} cm^{-2} s^{-1}, an additional component with a short decay time becomes apparent, and the fluorescence rate decreases. The fwhm of the fast component is identical with the instrument response

function of 400 ps. Attempts to block this component by different band-pass filters failed. Hence, we assign this signal to continuum generation ("white light") induced by a combination of several intensity effects such as spatial and temporal self-phase modulation, parametric four-wave mixing, stimulated Raman scattering, and thermal lens effects.[25,26] For comparison, the signal of pure water is given by the filled diamonds in Figure 2a. For small intensities the background signal has a long decay time, whereas at high intensities a characteristic scatter peak is detected; i.e., the continuum generation is caused by the solvent and not by the dissolved dye. The threshold photon flux $E_{P,qcw} = 2 \times 10^{26}$ cm^{-2} s^{-1} is clearly evident by the abrupt increase of the water signal and by the change of the decay curve.

To determine the portion S_{1av} of molecules in the S_1 state at the maximum fluorescence signal,[37] we calculate the excitation efficiency of TPE. It turns out that the portion of dye molecules in the S_1 state ($S_{1av} = 1-2\%$) is approximately the same as for OPE (see above); i.e., the deviation from the quadratic behavior is not caused by depletion of the S_0 state. It is important to mention that we have checked the TPE absorption cross section δ of Coumarin-120 in water, because the TPE cross sections of coumarins, which are given in the literature, were measured in alcohols but not in water. We observed an approximately 6-fold reduction in the excitation efficiency of Coumarin-120 in water compared to that of ethanol (δ(ethanol) $\approx 20 \times 10^{-50}$ cm^4 s)[21,22] at 700 nm; i.e., δ(water) $\approx 3 \times 10^{-50}$ cm^4 s. Additional proof of competing nonlinear solvent effects is the fact that the saturation of the TPE fluorescence is not specific for the dye Coumarin-120. Fluorescence saturation occurs also for the dyes Rhodamine 6G and Rhodamine B under the same conditions for TPE (data not shown). A direct comparison of experiments with a multichannel scaler (see below) for single-molecule detection of Rhodamine 6G by one-photon excitation (OPE)[14] and by two-photon excitation (TPE) demonstrates that the maximum fluorescence burst rates obtained by TPE are at least 1 order of magnitude smaller than those obtained by OPE. This is in agreement with results for the efficiency of fluorescence generation by OPE and TPE reported by Brakenhoff et al.[27]

We used FCS to investigate photobleaching for TPE. A typical autocorrelation curve of an aqueous Coumarin-120 solution (1 nM) is given in Figure 2b.

Figure 2c gives the calculated average number of molecules in the detection volume N(TPE) as a function of the applied laser power P.

From Figure 2c it is evident that N(TPE) remains approximately constant ($\approx$15) over the whole applied range of laser power. This indicates that photobleaching is negligible under the conditions used here.

3.2. Comparison of OPE and TPE for SMD. We compared the fluorescence fluctuations due to single-molecule transits through our detection volume by a multichannel scaler (MCS) using OPE at 350 nm and TPE at 700 nm. Poisson statistics predicts for such low concentrations that the number of molecules in the detection volume fluctuates predominantly between zero and one for a detection volume on the order of 1 fL. Let us define the signal-to-background ratio S/B by eq 4. We use a normalized signal count rate for a single-molecule transit, which is obtained by the ratio of the signal counts to the characteristic diffusion time τ_{Dx} determined by FCS.[1d] This definition allows a comparison of measurements with different experimental setups and is independent of the binning time of the multichannel scaler.

$$\mathrm{S/B} = \frac{\text{signal counts of a single molecule}/\tau_{Dx}}{\text{background counts per second}} \qquad (4)$$

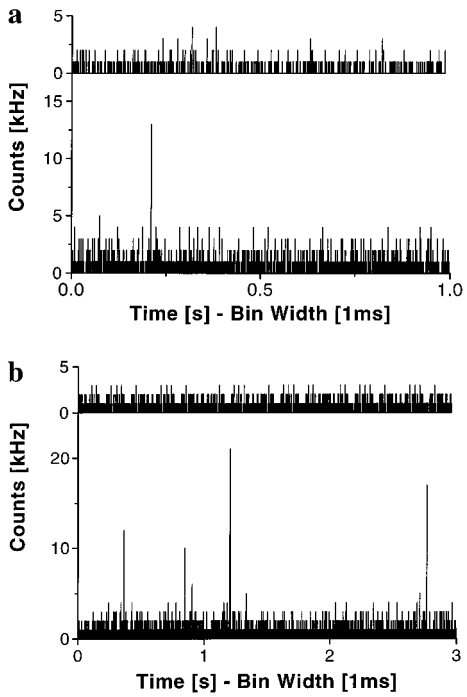

Figure 3. (a) Lower MCS trace: signal photon flow S_P with fluorescence bursts observed from Coumarin-120 (1×10^{-11} M in water) excited at 350 nm ($E_{P,qcw} = 7 \times 10^{22}$ cm^{-2} s^{-1}). Data acquisition was performed at a speed of 1000 data points per second (1 ms integration time). Upper MCS trace: signal photon flow of pure water. Parameters of the detection volume are the same as in Figure 1a. (b) Lower MCS trace: signal photon flow S_P with fluorescence bursts observed from Coumarin-120 (1×10^{-11} M in water) excited at 700 nm ($E_{P,qcw} = 2 \times 10^{26}$ cm^{-2} s^{-1}). Data acquisition was performed at a speed of 1000 data points per second (1 ms integration time). Upper MCS trace: signal photon flow of pure water. Parameters of the detection volume are the same as in Figure 2a.

Figure 3a,b shows two MCS traces of a 10^{-11} M aqueous Coumarin-120 solution for OPE and TPE: (a) $E_{P,qcw}$(OPE) $= 7 \times 10^{22}$ cm^{-2} s^{-1} (150 μW) and (b) $E_{P,qcw}$(TPE) $= 2 \times 10^{26}$ cm^{-2} s^{-1} (225 mW). In both cases the background signal of pure water is given in the upper trace.

Fluorescence burst rates up to 13 and 22 kHz at a background count rate of 380 and 430 Hz were obtained for OPE and TPE, respectively. The following signal-to-background ratios were obtained using the parameters for eq 4 given in the figure captions: S/B(TPE) = 1300 and S/B(OPE) = 400. According to Figure 2a, it should be possible to increase the signal-to-background ratio of TPE by a factor of 6, if $E_{P,qcw}$ is reduced to 1.5×10^{26} cm^{-2} s^{-1}, because the photon flux is just below the threshold for continuum generation resulting in an extreme low background rate of 70 Hz. Figures 1 and 3 prove the superior S/B ratio achieved for Coumarin-120 by TPE. The results obtained for Coumarin-120 are comparable to those of the frequently used dye Rhodamine-6G, where a S/B ratio of 1000[1d] for CW OPE and a S/B ratio of 400[14] for pulsed OPE are reported. This result must be seen in view of the fact that Rhodamine-6G has superior properties with respect to the absorption cross section, fluorescence lifetime, fluorescence quantum yield, and triplet quantum yield as well as photostability. The high S/B ratio for SMD of Coumarin-120 can be achieved due to the extreme low background level which has several reasons: (1) For OPE at 350 nm the Raman signal of the solvent is well separated spectrally from the fluorescence signal due to the large Stokes shift of 6750 cm^{-1} (maximum of fluorescence at 443 nm). (2) Also, for TPE at 700 nm Rayleigh and Raman scattered photons can be easily separated from the

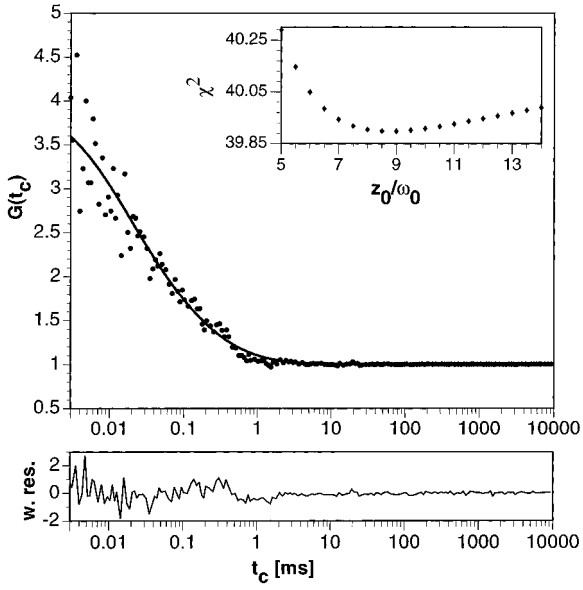

Figure 4. Normalized fluorescence autocorrelation curve $G(t_c)$ for an aqueous solution of Coumarin-120 (10^{-11} M): recorded data (black dots) and fitted curve (eq 1) with weighted residuals (w. res.).[30] Parameters of the fit with a background intensity of 430 Hz and a signal intensity of 480 Hz: base line = 0.9997, $N = 2.2 \times 10^{-3}$, $\tau_{D2} = 43\ \mu$s ($\omega_0 = 0.53\ \mu$m), $z_0/\omega_0 = 8.5$. The inset demonstrates the well-defined solution of eq 1 for the detection volume by the plot χ^2 (goodness of fit) vs the ratio z_0/ω_0.

fluorescence signal. On the other hand, it is obvious that the fluorescence bursts of Coumarin-120 are small compared to those of Rhodamine-6G, e.g., Rhodamine 6G up to 250 photons[14] and Coumarin-120 up to 25−30 photons (see Figure 3b). This result for Coumarin-120 is evidence for the low efficiency of OPE and TPE which limits the accuracy of the single-molecule detection. In the case of Rhodamine 6G there is a tradeoff between the number of detected photons and the signal-to-background ratio, because the Raman spectrum of the solvent and the fluorescence spectrum of the dye overlap. The efficiency of OPE of Rhodamine-6G is very high and is mainly limited by ground state depletion resulting in fluorescence saturation, while the background signal increases linearly with intensity and does not saturate. This effect leads to a dependence of the S/B ratio on the laser intensity, where the S/B ratio first increases with increasing intensity up to a maximum and then decreases due to saturation caused by ground state depletion. In case of Coumarin-120 the S/B ratio power dependence is completely different, because the excitation efficiency limits the S/B-ratio due to two-step photolysis for OPE or due to competing nonlinear effects in the solvent for TPE. We used TPE for single-molecule identification of Coumarin-120 for the following reasons: (1) The S/B ratio and the burst rates are higher than for OPE. (2) The high two-photon cross section δ of Coumarin-120 allows a more selective excitation by TPE than by OPE, since the one-photon cross section σ at 350 nm is quite small (5.8×10^{-17} cm^2). This is important for solutions of Coumarin-120, which may contain some fluorescing impurities (e.g., biomolecules).

3.3. Single-Molecule Identification by Time-Resolved Fluorescence Spectroscopy and TPE. *3.3.1. Determination of the Molecule Number by FCS.* To prove that we indeed observe single-molecule events, we measured the statistical average number of dye molecules in the detection volume via FCS for an aqueous Coumarin-120 solution (10^{-11} M). A typical normalized fluorescence autocorrelation curve is shown in Figure 4 with an amplitude $G(t_c = 0)$ of 3.7.

Using a diffusion coefficient $D = 8 \times 10^{-6}$ cm^2/s for Coumarin-120 in water[31] and the results of the fit given in Figure 4, a detection volume $V = 0.95$ fL is calculated. For such a small volume and a Coumarin-120 concentration of 10 pM an average number of molecules in the detection volume $N_V = 5.7 \times 10^{-3}$ is calculated. This result is in good agreement with a value of $N_A = 2.2 \times 10^{-3}$ obtained from the amplitude of the autocorrelation function $G(t_c{=}0)$ (see eq 1). For this average molecule number there is only a small probability to find more than one molecule at a time in the detection volume; i.e., we can be fairly sure to detect predominantly single-molecule events in our experiments. The inset in Figure 4 demonstrates the well-defined solution of eq 1 for the detection volume by the plot χ^2 (goodness of fit) vs the ratio z_0/ω_0.

3.3.2. Time-Correlated Single-Photon Counting and Maximum Likelihood Estimator. We measured repeatedly 100 successive signal decay curves with a constant number of photons at a quasi-CW photon flux of 2×10^{26} cm^{-2} s^{-1} to obtain fluorescence lifetimes of single molecules. The dead time of the electronics between two decay measurements within one sequence was smaller than 1 ms. Beside experiments in water (viscosity $\eta = 1$ cP at 293 K), we chose the more viscous solvent triacetin ($\eta = 28$ cP at 290 K[32]) to slow diffusion and to increase the observation time of each single molecule. This leads to an increased number of detected fluorescence photons per molecule transit. For one decay measurement 50 photons have been collected in water and 200 photons in the more viscous triacetin. As expected from the simultanously measured MCS and FCS data, most time-resolved signal decay curves showed a photon distribution that is typical for continuum generation and additional constant background (dark counts). Only in some measurements was an exponential signal decay observed that is typical for fluorescence as shown in Figure 5.

In the following statistical analysis of only a few detected photons in a single fluorescence burst, we need an optimal estimation procedure to determine the fluorescence lifetime. According to the Rao−Cramér theorem, a maximum likelihood estimator (MLE) is an efficient estimator,[10,33,34] because the estimates by a MLE reach the minimal limit for the variance. Furthermore, it has the lowest error or misclassification probability for small signal intensities.[35] Köllner et al.[10] used the MLE successfully for fluorescence pattern recognition. In single-molecule detection with TPE the number of emitted and detected fluorescence photons in experiments with single molecules is limited by the excitation efficiency, the diffusion time, the triplet lifetime, and the photostability of the dye. Recent experiments with time-resolved fluorescence detection analyze the fluorescence decay only partly[4,12,13,15] by disregarding its maximum. Therefore, we have developed an improved MLE algorithm, which uses the entire signal for data analysis. To obtain a signal curve appropriate for data analysis by the final eq 9, several steps are needed (eqs 5−8) to generate a realistic signal decay pattern M corresponding to a monoexponential fluorescence decay with a fluorescence lifetime τ. The fluorescence data obtained by time-correlated single-photon counting are accumulated in k channels of a finite measurement window T expressed as a reduced time window (in numbers of lifetimes) $\Gamma = T/\tau$. Assuming that the instrument response function (IRF) may be described by a δ pulse, the probability p_i of finding a count in channel i is then given by eq 5, considering $\Sigma p_i = 1$ according to a multinomial distribution.

$$p_i(\tau,T,k) = \left(\frac{e^{\Gamma/k} - 1}{1 - e^{-\Gamma}}\right) e^{-i\Gamma/k} \qquad (5)$$

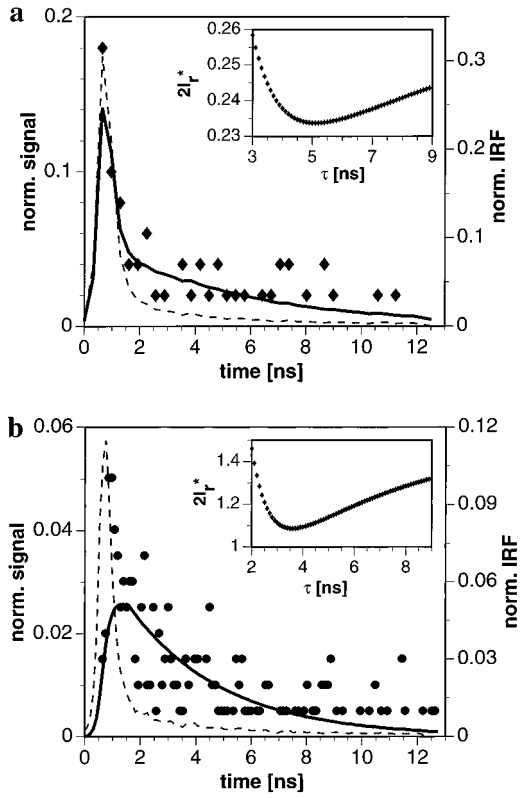

Figure 5. Normalized fluorescence decay curves (left axis) of single Coumarin-120 molecules in water (a) and triacetin (b). The dashed line represents the normalized instrument response function (IRF) (right axis). Five channels of the peak were used for convolution (eq 6). The fit (bold line) has been performed using the maximum likelihood estimator (eqs 8 and 9) with a variable scatter fraction γ and τ. A total of 119 channels have been used for data collection. The number of detected fluorescence photons N_F was calculated from γ and the total number of collected signal photons. The insets show the dependence of $2I_r^*$ on the fluorescence lifetime τ. (a) Water: $\tau_{MLE} = 5.1$ ns, $\gamma = 0.45$, $2I_r^* = 0.234$; $N_F = 28$. (b) Triacetin: $\tau_{MLE} = 3.4$ ns, $\gamma = 0.2$, $I_r^* = 1.103$, $N_F = 200$.

In eq 6 a more realistic fluorescence lifetime pattern C is generated by convolution of the probability R of the normalized instrument response function with the photon probability P of our lifetime model for a δ IRF (eq 5). Here u is the number of channels of the scatter decay curve R used for convolution. The scatter decay curve was obtained by continuum generation in the pure solvent at a high photon flux of the laser.

$$c_i(\tau,T,k) = (R \otimes P(\tau,T,k))_i = \sum_{j=0}^{\min(i,u)} r_j p_{i-j}(\tau,T,k) \qquad (6)$$

The fluorescence lifetime τ of Coumarin-120 ($\tau = 5$ ns in water[18]) is quite long compared to the time window of the measurement $T = 12.5$ ns, set by the repetition rate of the titanium:sapphire laser $1/f = 13.2$ ns. Hence, we must take the possibility into account that a dye molecule could have been excited by a previous pulse. Therefore, we sum over several pulses θ preceding the fluorescence photon, whereby the channel increment W is given by $W = k/(Tf)$. In our case it is sufficient to set $\theta = 3$. The final normalized fluorescence lifetime probability in channel i, $c'_i(\tau,T,k)$, is given in eq 7.

$$c_i'(\tau,T,k) = \sum_{\upsilon=0}^{\theta} c_{i+\upsilon W} \Big/ \sum_{i=1}^{k}\sum_{\upsilon=0}^{\theta} c_{i+\upsilon W} \qquad (7)$$

In our experiments each signal decay contains variable fractions γ of background signal due to continuum generation

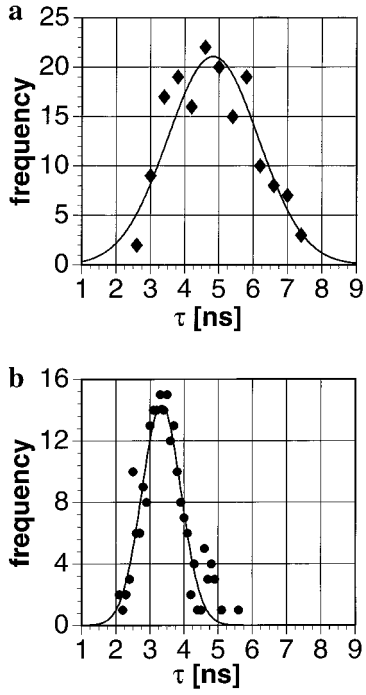

Figure 6. Histogram of the obtained fluorescence lifetimes τ calculated by the maximum likelihood estimator for single Coumarin-120 molecules in water and triacetin. Fitting to a Gaussian distribution yields the following average fluorescence lifetimes τ_{av} and standard deviations. (a) Water: $\tau_{av} = 4.8 \pm 1.2$ ns, bin width 0.4 ns. (b) Triacetin: $\tau_{av} = 3.3 \pm 0.6$ ns, bin width 0.1 ns.

L(k,T). Equation 8 gives the signal decay pattern $m_i(\tau,T,k,\gamma,L)$ in the channel i appropriate for eq 9 by the sum of the normalized distributions *L(k,T)* and $c'(\tau,T,k)$.

$$m_i(\tau,T,k,\gamma,L) = \gamma l_i(T,k) + (1-\gamma)c_i'(\tau,T,k) \qquad (8)$$

For pattern recognition signal patterns $M(\tau,T,k,\gamma,L)$ with variable fractions γ of background signal *L(k,T)* were generated by eq 8 in steps of $\tau = 100$ ps. On this two-dimensional parameter surface the optimal pattern was determined by the MLE in eq 9 on the basis of a minimum reduced $2I_r^*$ (Kullback−Leibler minimum discrimination information = $2I^*$).[10] Here n_i is the number of detected photons of the signal S in channel i, m_i is the probability of a distinct signal decay pattern that a count will fall in channel i, and f is the number of fitted parameters ($f = 2$). Normalization of $2I^*$ by the degrees of freedom ($k - 1 - f$) leads to the reduced $2I_r^*$, which is comparable to the reduced χ_r^2 known from least-squares estimators.

$$2I_r^* = \frac{2}{k-1-f}\sum_{i=1}^{k} n_i \ln\left(\frac{n_i}{Sm_i(\tau,T,k,\gamma,L)}\right) \qquad (9)$$

Two representative signal decays of Coumarin-120 in water and triacetin as well as the corresponding instrument response functions are given in Figure 5a,b. The insets show a cut through the $2I_r^*$ surface of the dependence on τ for an optimal fraction γ of background. The average number of photons detected in a burst of Coumarin-120 was 30 for water and 100 for triacetin. The distribution of the fluorescence lifetimes derived from individual bursts is shown in Figure 6a,b.

Fitting to a Gaussian distribution yields the following average fluorescence lifetimes τ_{av} and standard deviations: τ_{av}(water) $= 4.8 \pm 1.2$ ns and τ_{av}(triacetin) $= 3.3 \pm 0.6$ ns. These results are in good agreement with values obtained from separate

measurements at higher concentrations as well as with literature data: τ(water) = 5.0 ns[18] and τ(triacetin) = 3.4 ns.

4. Conclusions

We have shown the identification of a single fluorescent dye molecule in solution by time-resolved fluorescence spectroscopy with two-photon excitation due to its characteristic fluorescence lifetime. This appears to be the first single-molecule detection of a fluorescent dye by OPE and TPE, which has its one-photon S_0-S_1 absorption maximum in the near-UV. A high signal-to-background ratio of 1300 was achieved for TPE due to efficient rejection of background fluorescence and excitation light. SMD via TPE is free of multiphoton photolysis and has a high sensitivity. The high two-photon absorption cross section of Coumarin-120 allows a selective excitation. On the other hand, the efficiency of TPE is limited by competing nonlinear processes of the solvent. Experiments are underway to study the dependence of TPE efficiency for SMD in liquids on laser pulse width. The applicable laser intensity and thus the accuracy of SMD of Coumarin-120 by OPE are limited by two-step photolysis. The photostability of Coumarin-120 under the conditions of TPE was found to be sufficiently high. The results presented here offer new perspectives for such analytical applications in which fluorophores of small molecular weight are needed.

Acknowledgment. We are grateful to J. Troe and J. Wolfrum for generous support of this work. We thank M. Köllner, S. Hell, D. Schwarzer, and P. Vöhringer for fruitful discussions. We also thank K.-O. Greulich and S. Monajembashi for loaning us a Zeiss Ultrafluar 100× microscope objective. We would like to thank the Bundesministerium für Bildung und Forschung for financial support under grants 0310793 A and 0310806.

Appendix. Square Law of TPE

This appendix gives a derivation of eq 3 and treats the dependence of the time-averaged fluorescence photon flow F_P (s^{-1}) on the average photon flux $E_P(x,y,z)$ (cm^{-2} s^{-1}). Let us consider the collected fluorescence photon flow $F_P(t)$ of a solution excited by a mode-locked laser whose intensity is a periodic function in time. Equation A1 gives the quadratic dependence of the collected fluorescence photon flow $F_P(t)$ on the space- and time-dependent peak photon flux $E_{P,pk}(t,x,y,z)$,[20−22] where the parameters are defined in eqs 1−3.

$$F_P(t) = \alpha\delta c N_A \frac{\phi_F}{2}\int_v {E_{P,pk}}^2(t,x,y,z)\,\mathrm{CEF}(x,y,z)\,dx\,dy\,dz \quad \text{(A1)}$$

The photon flux profile of a focused laser beam is an axial (z) Lorentzian and radial (x, y) 2-dimensional Gaussian distribution (eqs A2a and A2b),[23]

$$E_P(x,y,z) = E_{P,0}\frac{{\omega_0}^2}{\omega(z)^2}\exp(-2(x^2+y^2)/\omega(z)^2) \quad \text{(A2a)}$$

$$\omega(z)^2 = {\omega_0}^2 + \left(\frac{\lambda}{n_D\pi\omega_0}\right)^2 z^2 \quad \text{(A2b)}$$

where $E_{P,0}$ is the photon flux at the center of the laser beam waist on the optical axis, ω_0 is the $1/e^2$ radius of the Gaussian laser beam in the radial direction (x,y) at $z = 0$, n_D is the refractive index of the medium, and λ is the laser wavelength. In eq A3 the molecular detection efficiency MDE = ${E_{P,pk}}^2$ × CEF is approximated by a squared 3-dimensional Gaussian fluorescence distribution $W^2(x,y,z)$.[23]

$$MDE = {E_{P,0}}^2\exp(-4(x^2+y^2)/{\omega_0}^2)\times \exp(-4(z^2)/{z_0}^2) = {E_{P,0}}^2 W^2(x,y,z) \quad \text{(A3)}$$

The photon flux $E_{P,0}$ at the focal center of the Gaussian beam ($z = 0$) can be calculated by the $1/e^2$ radius ω_0 and the total laser power $P(W)$ given by eq A4. The radius ω_0 can be determined by FCS (see Section 2.2) while the total power of the focused Gaussian beam is measured by a power meter integrating over the entire beam, $A = \int\exp(-(x^2+y^2)/{\omega_0}^2)\,dx\,dy = (\pi/2){\omega_0}^2$.[24]

$$E_{P,0} = \frac{P}{(\pi/2){\omega_0}^2}\frac{\lambda}{hc_1} \quad \text{(A4)}$$

In eq A4 h is Planck's constant and c_l is the velocity of light.

TPE was performed by a mode-locked laser. The periodic nature of this pulse train is defined by the repetition rate f of the laser and the excitation pulse width τ_p (fwhm). However, we can only measure a time-averaged quasi-CW photon flux $E_{P,qcw}$ by a power meter. Since TPE is a nonlinear process, the difference between the squared photon flux ${E_P}^2(t)$ and the square of the photon flux $E_P(t)^2$ has to be taken into account by defining a two-photon "advantage" factor g.[22] This factor is determined by the second-order temporal coherence of the laser pulse with respect to a specified pulse shape and by the duty cycle $f\tau_p$. When sech^2 temporal-shaped pulses are assumed, g is given by eq A5.

$$g = \frac{{E_P}^2(t)}{(E_P(t))^2} = \frac{\int_{-\infty}^{\infty} f(E_P\,\mathrm{sech}^2(1.76t/\tau_p))^2\,dt}{(\int_{-\infty}^{\infty} fE_P\,\mathrm{sech}^2(1.76t/\tau_p)\,dt)^2} = \frac{0.588}{f\tau_p} \quad \text{(A5)}$$

If time-averaged signals are used for data analysis, the time-averaged fluorescence photon flow F_P must be studied as a function of the time-averaged quasi-CW photon flux $E_{P,qcw}$ analogous to eq A1. Combining eqs A1, A3, and A5, eq 3 can be derived.

References and Notes

(1) (a) Eigen, M.; Rigler, R. *Proc. Natl. Acad. Sci. U.S.A.* **1994**, *91*, 5740. (b) Rigler, R. J. *Biotechnology* **1995**, *41*, 177. (c) Rigler, R.; Mets, Ü. *SPIE Proc.* **1992**, *1921*, 239. (d) Mets, Ü.; Rigler, R. *J. Fluoresc.* **1994**, *4*, 259.

(2) Keller, R. A.; Ambrose, W. P.; Goodwin, P. M.; Jett, J. H.; Martin, J. C.; Ming, W. *Appl. Spectrosc.* **1996**, *50*, 7.

(3) (a) Nie, S.; Chiu, D. T.; Zare, R. N. *Science* **1994**, *266*, 1018. (b) Nie, S.; Chiu, D. T.; Zare, R. N. *Anal. Chem.* **1995**, *67*, 2849.

(4) (a) Jett, J. H.; Keller, R. A.; Martin, J. C.; Marrone, B. L.; Moyzis, R. K.; Ratliff, R. L.; Seitzinger, N. K.; Shera, E. B.; Stewart, C. C. *J. Biomol. Struct. Dyn.* **1989**, *7*, 301. (b) Shera, E. B.; Seitzinger, N. K.; Davis, L. M.; Keller, R. A.; Soper, S. A. *Chem. Phys. Lett.* **1990**, *174*, 553.

(5) Rigler, R.; Mets, Ü.; Widengren, J.; Kask, P. *Eur. Biophys. J.* **1993**, *2*, 169.

(6) Mertz, J.; Xu, C.; Webb, W. W. *Opt. Lett.* **1995**, *20*, 2532.

(7) Plakhotnik, T.; Walser, D.; Pirotta, M.; Renn, A.; Wild, U. P. *Science* **1996**, *271*, 1703.

(8) Berland, K. M.; So, P. T. C.; Gratton, E. *Biophys. J.* **1995**, *68*, 694.

(9) (a) Denk, W.; Strickler, J. H.; Webb, W. W. *Science* **1990**, *248*, 73. (b) Pawley, J. B., Ed. *Handbook of Biological Confocal Microscopy*; Plenum Press: New York, 1995. (c) Hänninen, P. E.; Schrader, M.; Soini, E.; Hell, S. W. *Bioimaging* **1995**, *3*, 70. (d) So, P. T. C.; French, T.; Yu, W. M.; Berland, K. M.; Dong, C. Y.; Gratton, E. *Bioimaging* **1995**, *3*, 49.

(10) (a) Köllner, M.; Wolfrum, J. *Chem. Phys. Lett.* **1992**, *200*, 199. (b) Köllner, M. *Appl. Opt.* **1993**, *32*, 806. (c) Köllner, M.; Fischer, A.; Arden-Jacob, J.; Drexhage, K. H.; Müller, R.; Seeger, S.; Wolfrum, J. *Chem. Phys. Lett.* **1996**, *250*, 355.

(11) Lee, Y.-H.; Maus, R. G.; Smith, B. W.; Wineforder, J. D. *Anal. Chem.* **1994**, *66*, 4142.

(12) Sauer, M.; Drexhage, K. H.; Zander, C.; Wolfrum, J. *Chem. Phys. Lett.* **1996**, *254*, 223.

(13) Soper, S. A.; Davis, L. M.; Shera, E. B. *J. Opt. Soc. Am. B* **1992**, *9*, 1761.

(14) Zander, C.; Sauer, M.; Drexhage, K. H.; Ko, D.-S.; Schulz, A.; Wolfrum, J.; Brand, L.; Eggeling, C.; Seidel, C. A. M. *Appl. Phys. B* **1996**, *63*, 517−523.

(15) Müller, R.; Zander, C.; Sauer, M.; Deimel, M.; Ko, D.-S.; Siebert, S.; Arden-Jacob, J.; Deltau, G.; Marx, N. J.; Drexhage, K. H.; Wolfrum, J. Submitted to *Chem. Phys. Lett.*

(16) (a) Seidel, C. A. M. Thesis, Ruprecht-Karls-Universität, Heidelberg, 1992. (b) Eggeling, C. Diploma thesis, Universität Göttingen, 1996.

(17) Drexhage, K. H. In *Topics in Applied Physics*; Schäfer, F. P., Ed.; Springer: Berlin, 1973; Vol. 1 (Dye lasers).

(18) Seidel, C. A. M.; Schulz, A.; Sauer M. H. M. *J. Phys. Chem.* **1996**, *100*, 5541.

(19) Glossary of terms used in photochemistry: Braslavsky, S. E.; Houk, K. N. *Pure Appl. Chem.* **1988**, *60*, 1055.

(20) Göppert-Mayer, M. *Ann. Phys.* **1931**, *9*, 273.

(21) Fischer, A.; Cremer, C.; Stelzer, E. H. K. *Appl. Opt.* **1995** *34*, 1989.

(22) (a) Xu, C.; Webb, W. W. *J. Opt. Soc. Am. B* **1996**, *13*, 481. (b) Xu, C.; Williams, R. M.; Zipfel, W.; Webb, W. W. *Bioimaging* **1996**, *4*, 198.

(23) Quian, H.; Elson, E. L. *Appl. Opt.* **1991**, *30*, 1185.

(24) Siegman, A. E., *Lasers*; University Science Books: Mill Valley, CA, 1986.

(25) Alfano, R. R., Ed. *The Supercontinuum Laser Source*; Springer: New York, 1989.

(26) Friedrich, D. M. *J. Chem. Educ.* **1982**, *59*, 472.

(27) (a) Brakenhoff, G. J.; Müller, M.; Ghauharali, R. I. *J. Microsc.* **1996**, *183*, 140. (b) Brakenhoff, G. J.; Müller, M.; Squier, J. *J. Microsc.* **1995**, *179*, 253.

(28) (a) Elson, E. L.; Magde, D. *Biopolymers* **1974**, *13*, 1. (b) Magde, D.; Elson, E. L.; Webb, W. W. *Biopolymers* **1974**, *13*, 29. (c) Thompson, N. L. In *Topics in Fluorescence Spectroscopy*; Lakowicz, J. R., Ed.; Plenum Press: New York, 1991; Vol. 1, p 337.

(29) (a) Widengren, J.; Mets, Ü.; Rigler, R. *J. Phys. Chem.* **1995**, *99*, 13368.

(30) Koppel, D. E. *Phys. Rev. A* **1974**, *10*, 1938.

(31) The diffusion coefficient used here was calculated in analogy to compounds of comparable molecular weight and molecular shape as given in: *Landoldt Börnstein II*, 6th ed.; Springer: Heidelberg, 1969; Vol. 5, p 666.

(32) *Handbook of Chemistry and Physics*. 58th ed.; CRC Press: Cleveland, OH, 1977.

(33) Hall, P.; Selinger, P. *J. Chem. Phys.* **1981**, *85*, 2941.

(34) Tellinghuisen, J.; Goodwin, P. M.; Ambrose, W. P.; Martin, J. C.; Keller, R. A. *Anal. Chem.* **1994**, *66*, 64.

(35) Kotze, T. J. v. W.; Gokhale, D. V. *J. Stat. Comput. Simul.* **1980**, *12*, 1.

(36) Mathies, R., A.; Peck, K.; Stryer, L. *Anal. Chem.* **1990**, *62*, 1786.

(37) The portion of dye molecules in S_1 state S_{1av} is calculated from the steady state solution of ref 36 using standard kinetic rate constants for singlet depopulation (2×10^8 s^{-1}), intersystem crossing (1×10^6 s^{-1}), and triplet depopulation (4×10^5 s^{-1}).[29] The excitation rate was obtained using a OPE absorption cross section σ of 5.8×10^{-17} cm^2 ($\epsilon = 15\,000$ M^{-1} cm^{-1}) or a TPE absorption cross section δ of 3×10^{-50} cm^4 s.

(38) (a) Rosenthal, I. *Opt. Commun.* **1978**, *24*, 164. (b) Soper, S. A.; Nutter, H. L.; Keller, R. A.; Davis, L. M.; Shera, E. B. *Photochem. Photobiol.* **1993**, *57*, 972. (c) Widengren, J.; Rigler, R. *Bioimaging* **1996**, *4*, 149. (d) Eggeling, C.; Widengren, J.; Rigler, R.; Seidel, C. A. M. Manuscript in preparation.

(39) Dempster, D. N.; Morrow, T.; Quinn, M. F. *J. Photochem.* **1973/74**, *2*, 329.